

Three-carbazole-armed host materials with various cores for RGB phosphorescent organic light-emitting diodes†

Shi-Jian Su,^{*a} Chao Cai^b and Junji Kido^{*b}

Received 24th August 2011, Accepted 23rd November 2011

DOI: 10.1039/c2jm14151e

A series of three-carbazole-armed host materials containing various arylene cores, like benzene (1,3,5-tris(3-(carbazol-9-yl)phenyl)-benzene, TCPB), pyridine (2,4,6-tris(3-(carbazol-9-yl)phenyl)-pyridine, TCPY), and pyrimidine (2,4,6-tris(3-(carbazol-9-yl)phenyl)-pyrimidine, TCPM), were developed for red, green, and blue phosphorescent organic light-emitting diodes (OLEDs). An intramolecular charge transfer was observed for TCPY and TCPM with heterocyclic cores of pyridine and pyrimidine, giving bathochromic shifts in the photoluminescent spectrum and reduced energy band gaps in comparison with TCPB with a benzene core. In addition, lower energy singlet and triplet excited states, reduced lowest unoccupied molecular orbital (LUMO) energy level, smaller singlet–triplet exchange energy (ΔE_{ST}), and improved bipolarity were also achieved with introducing heterocycles of pyridine and pyrimidine instead of benzene. In contrast to the slightly decreased triplet energy (E_T), a significantly decreased ΔE_{ST} was achieved by introducing heterocycles of pyridine and pyrimidine as the core, and the more nitrogen atoms in the central heterocycle, the smaller ΔE_{ST} is achieved. Reduced driving voltages were achieved for the green and red phosphorescent OLEDs by utilizing TCPY and TCPM as the host due to their decreased ΔE_{ST} and lower-lying LUMO energy level, proving that more carriers must be injected into the emitting layer through the host molecules rather than direct carrier trapping by the dopant. Moreover, improved efficiency and suppressed efficiency roll-off were also achieved for the green and red phosphorescent OLEDs based on TCPY and TCPM due to their improved bipolarity and thus improved carrier balance.

Introduction

Phosphorescent organic light-emitting diodes (OLEDs) have attracted tremendous attention since nearly 100% internal quantum efficiency of electroluminescence is readily achieved by harvesting both electro-generated singlet and triplet excitons by fast intersystem crossing for phosphorescence emission from the triplet excited states of the transition metal-centered phosphors.^{1–4} For those phosphorescent OLEDs, phosphorescent emitters are normally doped into an appropriate host material as an emitting layer (EML) to avoid self-aggregation quenching and

triplet–triplet annihilation. As a matrix material for the phosphorescent emitters, it is essential that the triplet energy (E_T) of the host is higher than that of the emitter in order to facilitate energy transfer from the host to the phosphorescent emitter and to prevent energy back transfer from the guest to the host, regardless of the emitting colors.^{5,6} To meet this requirement, most effort have been made to develop host materials with limited π -conjugation. For example, triphenyl silyl has been introduced into the hosts as a building block to break their π -conjugation,^{7–9} and several organosilicon compounds have been reported having ultra-high triplet energies.¹⁰ However, the charge hopping in the EML generally occurred between the adjacent dopant molecules due to their ultrawide energy band gaps (E_g) to give increased operating voltage.¹¹ As thus, another requirement for a host material is its carrier transport property. An optimized carrier recombination in the EML is indispensable to give a high efficiency. Over the years, many host materials have been described with building blocks of well-known electron donors of carbazole^{12–16} and triphenylamine.¹⁷ In general, the electron mobility of those hosts is much lower than the hole mobility because of the fact that they mainly consist of strong electron donors like aromatic amine or carbazole. Besides the building blocks of electron donors, introduction of electron acceptors like benzimidazole,^{18–21} phosphine oxide,^{22,23} triazine,^{24–26} and

^aInstitute of Polymer Optoelectronic Materials and Devices, State Key Laboratory of Luminescent Materials and Devices, South China University of Technology, Guangzhou, 510640, China. E-mail: mssjsu@scut.edu.cn

^bDepartment of Organic Device Engineering, Graduate School of Science and Engineering, Yamagata University, 4-3-16 Jonan, Yonezawa, Yamagata, 992-8510, Japan. E-mail: kid@yz.yamagata-u.ac.jp

† Electronic supplementary information (ESI) available: Synthetic procedure and spectroscopic characterizations of the compounds TCPB, TCPY, and TCPM; molecular structures of DCzPB, 26DCzPPy, 24DCzPPy, 24DCzPPm, and 46DCzPPm; molecular structures and acronyms of the materials used for device fabrication; PL spectra of the co-deposited films; JVL and EL characteristics of the RGB phosphorescent OLEDs. See DOI: 10.1039/c2jm14151e

oxadiazole,²⁷ was proven to be an effective route to give host materials with improved electron mobility. Most recently, some host materials with building blocks of both electron donor and acceptor, called bipolar host materials, were developed with improved bipolarity.^{28–34} However, few work reported on the structure-property relationship according to the electron donor and acceptor, especially for the phosphorescent OLEDs utilizing blue, green, and red phosphorescent emitters.

In this article, we report on a series of three-carbazole-armed host materials composed of carbazole as the periphery and triphenyl arylene as the core. They are different from each other in chemical structure and electron affinity of the central arylens, like benzene, pyridine, and pyrimidine. Their carrier mobilities and energy levels, including the highest occupied molecular orbital (HOMO), the lowest unoccupied molecular orbital (LUMO), singlet and triplet energies, and their energy difference, can be effectively tuned by the different central arylens. Red, green, and blue phosphorescent OLEDs were fabricated with well-known triplet emitters of tris(1-phenylisoquinolinolato-*C*²,*N*)iridium(III) (Ir(piq)₃), *fac*-tris(2-phenylpyridine) iridium (Ir(PPy)₃), and iridium(III) bis(4,6-(di-fluorophenyl)pyridinato-*N*,*C*²) picolinate (FIrpic), respectively. The effects of the central arylens on their photophysical properties, electron/hole mobilities, and electroluminescence performances were studied comprehensively. In addition, compared with the host materials with the same arylene core and only two phenyl carbazole arms, the current three-carbazole-armed host materials exhibit improved bipolarity and thus an improved carrier balance and device performance.

Results and discussion

Syntheses of 1,3,5-tris(3-(carbazol-9-yl)phenyl)-benzene (TCPB), 2,4,6-tris(3-(carbazol-9-yl)phenyl)-pyridine (TCPY), and 2,4,6-tris(3-(carbazol-9-yl)phenyl)-pyrimidine (TCPM) are outlined in Scheme 1. The intermediates of 1,3,5-tri(*m*-bromophenyl)benzene (**1**),³⁵ 9-(3-bromophenyl)-carbazole (**3**),²⁸ and 9-(4,4,5,5-tetramethyl-1,3,2-dioxaborolan-2-yl)phenyl)-carbazole (**4**)²⁸ were synthesized according to the literature procedures. 2,4,6-Tris(3-bromophenyl)pyridine (**2**) was synthesized with a condensation reaction of 3-bromobenzaldehyde and 3-bromoacetophenone in the presence of KOH and concentrated NH₄OH. TCPB and TCPY were synthesized with a palladium catalyzed amination reaction in yields of 89% and 91%, respectively. TCPM was synthesized with a palladium catalyzed Suzuki coupling reaction in yield of 89%. All the developed host materials were purified by silica gel chromatography and then repeated thermal gradient vacuum sublimation before characterization and device fabrication.

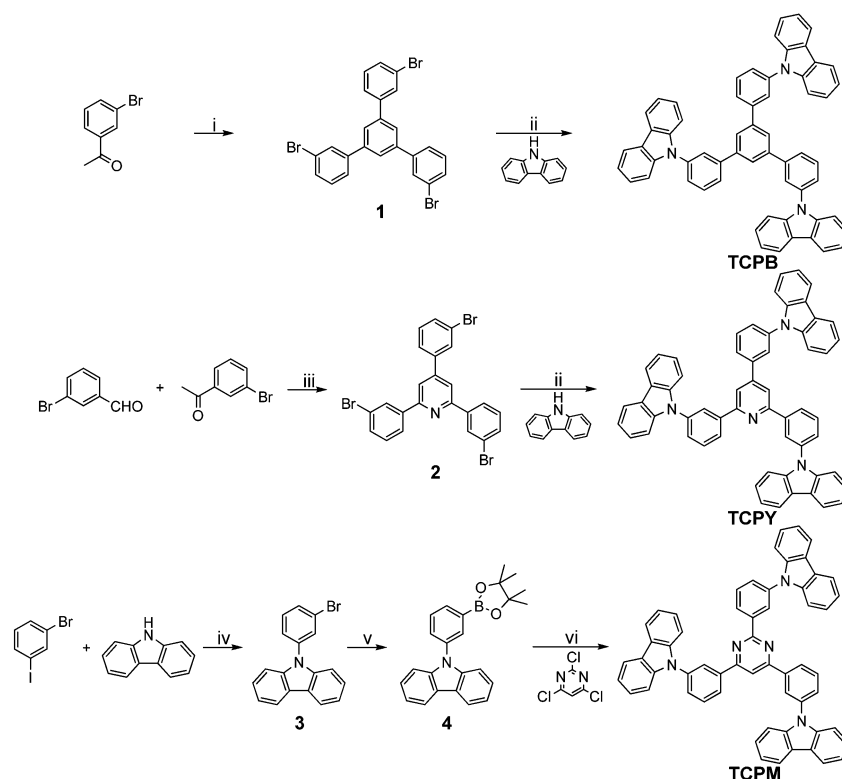
UV-vis absorption and steady-state photoluminescence (PL) spectra for the vacuum deposited films (60 nm) of the developed host materials on quartz substrates were measured at room temperature (Fig. 1a). Their UV-vis absorption spectra are quite similar with peaks and shoulders at 285, 296, 330, and 345 nm that can be attributed to the π - π^* transitions of the carbazole chromophore on the periphery. The absorption peaks at around 244 nm and the shoulders at 265 nm can be attributed to the π - π^* and n - π^* transitions of the central triphenyl arylens, respectively. However, compared with TCPB with a benzene

core, the absorptions in the range of 350 and 400 nm for TCPY and TCPM slightly increase with introducing heterocycles of pyridine and pyrimidine as the core instead of the central benzene. This can be attributed to strong electron affinity of pyridine and pyrimidine and thus intramolecular charge transfer formed between the central heterocycle and the outer carbazole. As a result, from their absorption edges, relatively narrower energy band gaps (E_g) of 3.42 and 3.15 eV are obtained for TCPY and TCPM, respectively, compared with 3.46 eV for TCPB (Table 1). In addition, the more nitrogen atoms in the heterocyclic core, the narrower E_g is obtained due to the improved electron affinity of the central arylene and thus stronger intramolecular charge transfer.

The PL spectrum of TCPB exhibits peaks at 351, 380 and 400 nm. In contrast, the PL spectra of TCPY and TCPM are featureless and peak at 415 and 436 nm, respectively. The bathochromic shift of the PL spectrum is clearly found by introducing heterocycles of pyridine and pyrimidine as the core instead of the central benzene of TCPB, the more nitrogen atoms present in the heterocyclic core, the longer the bathochromic shift obtained. This phenomenon can be also attributed to the intramolecular charge transfer of the compounds containing a heterocyclic core.

HOMO energy levels of TCPB, TCPY, and TCPM which are determined by atmospheric photoelectron spectroscopy are slightly influenced by the change of the central arylene. In contrast, lower-lying LUMO energy levels were achieved by introducing heterocycles of pyridine and pyrimidine with stronger electron affinities as the core instead of the central benzene. The more nitrogen atoms present in the central heterocyclic arylene, the stronger the electron affinity and the lower-lying LUMO energy levels are achieved.

To obtain the E_{TS} of the developed host materials, extremely long decay components of their transient photoluminescence, lasting for ~ 10 ms, were recorded at $T = 4.2$ K. Fig. 1b shows two time-resolved emission spectra for each film. One is the emission spectrum obtained in the whole range ($0 < t < 10$ ms) (black lines), comprising both singlet and triplet emissions. The other is the emission spectrum of the delayed component ($2 \text{ ms} < t < 10 \text{ ms}$) (grey lines), generally consisting of triplet emission, also called phosphorescence spectrum of the corresponding host material. TCPB exhibits the highest energy phosphorescence peak ($S_0^v = 0 \leftarrow T_1^v = 0$) at 466 nm, corresponding to E_T of 2.66 eV. Compared with a general host material of *N,N'*-dicarbazolyl-4,4'-biphenyl (CBP) ($E_T = 2.56$ eV), the higher E_T can be attributed to the break of π conjugation when the central arylens are combined with each other at their *meta*-positions (refer to the combination sites). With introducing pyrimidine instead of the central benzene, slightly decreased E_T of 2.64 eV is obtained for TCPM with the highest energy phosphorescence peak at 470 nm. Different from the emission spectra of the delayed components of TCPB and TCPM, there is a strong emission between 380 and 460 nm for the delayed component of TCPY, which can be attributed to its delayed fluorescence. Besides the delayed fluorescence, it also shows phosphorescence at wavelengths longer than 460 nm with the highest energy phosphorescence peak at 472 nm, corresponding to E_T of 2.63 eV. Compared with the host materials with the same arylene core and only two phenyl carbazole arms,³⁴ E_T of the current hosts with three phenyl carbazole arms is slightly lower, which can be attributed



Scheme 1 Synthetic routes of TCPB, TCPY, and TCPM. Reagents and conditions: (i) SiCl_4 , anhydrous ethanol, 0–25 °C; (ii) PdCl_2 , tris(*tert*-butyl)phosphine, sodium *tert*-butoxide, anhydrous *o*-xylene, 120 °C; (iii) KOH, ethanol, concentrated NH_4OH , reflux; (iv) Cu, K_2CO_3 , DMF, 130 °C; (v) bis(pinacolato)diboron, $\text{Pd}_2(\text{dba})_3$, KOAc, PCy_3 , dioxane, 80 °C; (vi) $\text{PdCl}_2(\text{PPh}_3)_2$, 2 M K_2CO_3 , 1,4-dioxane, 90 °C.

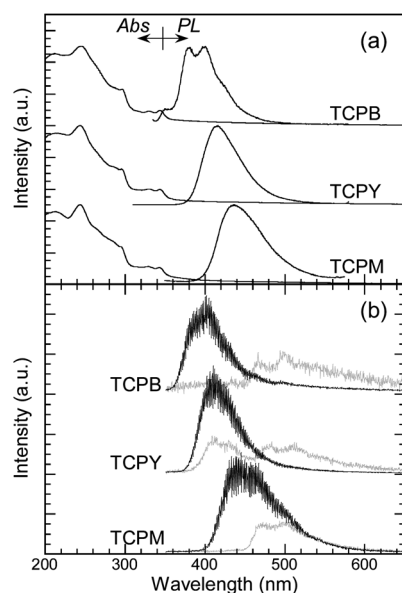


Fig. 1 (a) Room temperature UV-vis absorption and steady-state photoluminescence spectra for the vacuum-deposited films of TCPB, TCPY, and TCPM on quartz substrates. (b) Time-resolved emission spectra for the vacuum-deposited films of TCPB, TCPY, and TCPM excited by a nitrogen laser ($\lambda = 337$ nm, 50 Hz, 800 ps) at $T = 4.2$ K. Black lines: Emission spectra in the whole range ($0 < t < 10$ ms). Grey lines: Emission spectra of the delayed components, generally called phosphorescence spectra ($2 \text{ ms} < t < 10$ ms).

to more delocalized π conjugation in these molecules. Different from the fluorescence spectra, very slight bathochromic shift in phosphorescence was found with introducing one or two nitrogen atoms in the central arylene, resulting in slightly lower E_T . Since π conjugations of the current hosts are similar to each other, compared with TCPB, the slightly reduced E_T of TCPY and TCPM can be attributed to the intramolecular charge transfer formed between the heterocyclic core and the carbazole periphery.

Compared with the phosphorescence spectra, the prompt and stronger emissions at shorter wavelengths are due to the fluorescence of the host materials, which are almost consistent with those measured at room temperature. From the highest energy fluorescence peaks ($S_0^{v=0} \leftarrow S_1^{v=0}$), singlet energies (E_S) of TCPB, TCPY, and TCPM can be estimated as 3.26, 3.02, and 2.82 eV, respectively (Table 2). In general, a host material should have an exchange energy as small as possible to allow for charge injection into the host and efficient triplet emission from a dispersed triplet emitter.¹⁶ Here, the energy difference (ΔE_{ST}) between the singlet and triplet emission transitions is taken as an estimate for the exchange energy. Compared with TCPB ($\Delta E_{ST} = 0.60$ eV), a decrease of ΔE_{ST} by 0.21 eV was achieved for TCPY by introducing a pyridine core instead of the central benzene. In addition, with introducing one more nitrogen atom in the central pyridine core, further decreased ΔE_{ST} of 0.18 eV was achieved for TCPM, which is much smaller than those of most previously reported host materials.^{16,34} Compared with the slightly reduced E_T , the significantly decreased ΔE_{ST} achieved

Table 1 Physical and photophysical properties of TCPB, TCPY, and TCPM. Also shown is the data for the host materials with the same arylene core and two phenyl carbazole arms, like DCzPB, 26DCzPPy, 24DCzPPy, 24DCzPPm, and 46DCzPPm.³⁴ Their molecular structures are shown in Scheme S1 (see ESI†)

Materials	T_g^a (°C)	T_m^a (°C)	T_d^b (°C)	λ_{PL}^c (nm)	E_g^d (eV)	HOMO ^e (eV)	LUMO ^f (eV)
TCPB	146	261	518	351, 380, 400	3.46	6.16	2.70
DCzPB	101	276	452	352, 378, 400	3.48	6.08	2.60
TCPY	149	288	511	415	3.42	6.19	2.77
26DCzPPy	102	230	455	387	3.40	6.05	2.65
24DCzPPy	106	n.d.	466	401	3.38	6.15	2.77
TCPM	155	310	509	436	3.15	6.17	3.02
24DCzPPm	108	185	454	426	3.17	6.19	3.02
46DCzPPm	107	175	466	439	3.13	6.19	3.06

^a Glass transition temperature (T_g) and melting temperature (T_m) obtained from differential scanning calorimetry (DSC) measurements.

^b Decomposition temperature (T_d) obtained from thermogravimetric analysis (TGA). ^c Photoluminescence (PL) spectra of vacuum-deposited films on quartz substrates at room temperature. ^d Energy band gap (E_g) from the lowest-energy absorption edge of the UV-vis absorption spectra. ^e HOMO energy level determined by atmospheric ultraviolet photoelectron spectroscopy (Rikken Keiki AC-3). ^f LUMO energy level calculated from HOMO and E_g .

with introducing heterocycles as the core indicates that introducing both electron donors and acceptors as building blocks of a host material may be an effective route to give attractive candidates for phosphorescent OLEDs with reduced driving voltage as well as good triplet exciton confinement.

Besides photophysical properties, their thermal properties, like glass transition temperatures (T_g) and melting temperatures (T_m) are also influenced by the change of the arylene core. Improved T_g and T_m are achieved for the host materials with one or two nitrogen atoms in the central arylene, and it can be attributed to the increase of polarity and thus stronger molecular interaction. In addition, all they show a T_g higher than 140 °C, which are over 40 °C higher than those of the host materials with the same arylene core and two phenyl carbazole arms (Table 1).³⁴ In comparison, a general host CBP shows a crystalline behavior, and no T_g was detected in the DSC.³⁶ The high T_g values of the current three-carbazole-armed hosts prove the high morphologic stability of the amorphous phase in a deposited film, which is a prerequisite for their applications in OLEDs.

DFT calculations were performed using the Gaussian suite of programs (Gaussian 03W) for the structures of TCPB, TCPY, and TCPM. As shown in Fig. 2, HOMOs of all the molecules are mainly located at the carbazole periphery. In contrast, their LUMOs are mainly located at the central triphenyl arylene skeleton among the outer carbazoles. As a result, lower-lying LUMO energy levels are obtained by introducing heterocycles of pyridine and pyrimidine as the core instead of the central benzene, and the more nitrogen atoms in the heterocyclic, the lower-lying LUMO energy level is obtained. In comparison, their

HOMO energy levels are slightly influenced by the change of the central arylene. Moreover, the trends of the calculated energy levels are conceivably consistent with the experimental ones, although the exact values are somewhat different.

Their triplet energies are calculated from the difference of their ground state (S_0) and triplet excited state (T_1) energies. The calculated triplet energies ($T_1 - S_0$) of TCPB, TCPY, and TCPM are 2.98, 2.87, and 2.81 eV, and it further proves that introduction of heterocycle as the core in combination of carbazole periphery induces lower triplet energy. As shown in Table 2, the energy difference (ΔE) between the calculated E_g and ($T_1 - S_0$) is taken as an estimate for the energy difference between the singlet and triplet transitions. Similar to the experimental ΔE_{ST} , ΔE of TCPB with a benzene core is the largest one among these hosts, and smaller ΔE is achieved with introducing one or two nitrogen atoms in the central benzene. Moreover, consistent with the experimental result, ΔE of the current hosts with three phenyl carbazole arms is smaller than the hosts with the same arylene core and two phenyl carbazole arms, and ΔE of TCPM is the smallest one among these hosts.³⁴

As a host material for a triplet emitter, its triplet excited state should be higher than that of the triplet emitter to prevent reverse energy transfer from the guest to the host. It seems in contradiction with this requirement since decreased E_T is obtained by introducing pyridine or pyrimidine as the core of the host in comparison with the benzene core. To verify their triplet exciton confinement ability, well-known red, green, and blue triplet emitters of Ir(piq)₃, Ir(PPy)₃, and FIrpic were co-deposited with the current hosts for transient PL decay measurements.

Table 2 Singlet energies (E_S , measured as $S_0^{v=0} \leftarrow S_1^{v=0}$ at 4.2 K), triplet energies (E_T , measured as $S_0^{v=0} \leftarrow T_1^{v=0}$ at 4.2 K), and singlet–triplet energy difference ($\Delta E_{ST} = E_S - E_T$) for TCPB, TCPY, and TCPM

Materials	E_S (eV)	E_T (eV)	ΔE_{ST} (eV)	E_g^a (eV)	$T_1 - S_0^a$ (eV)	ΔE^a (eV)
TCPB	3.26	2.66	0.60	4.03	2.98	1.05
TCPY	3.02	2.63	0.39	3.59	2.87	0.75
TCPM	2.82	2.64	0.18	3.24	2.81	0.43

^a Calculated energy band gaps ($E_g = \text{HOMO} - \text{LUMO}$), triplet energies ($T_1 - S_0$), and energy differences between E_g and ($T_1 - S_0$) ($\Delta E = E_g - (T_1 - S_0)$).

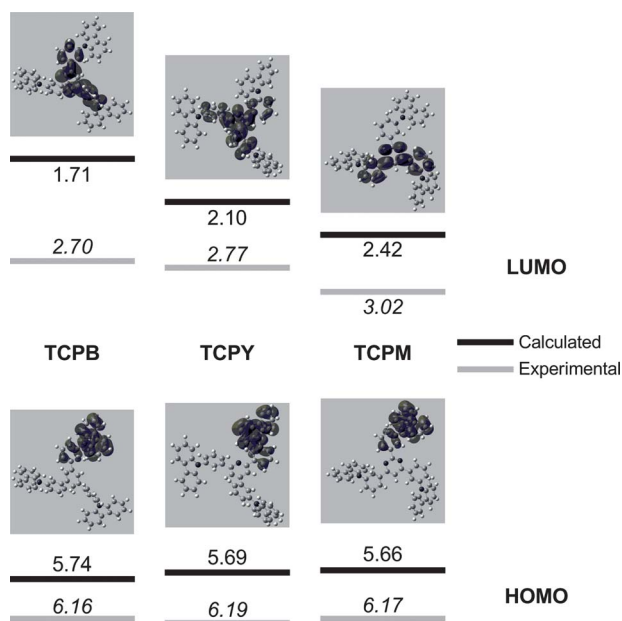


Fig. 2 The calculated spatial distributions and energy levels (eV) of HOMO and LUMO for TCPB, TCPY, and TCPM. Also shown the experimental HOMO and LUMO energy levels (eV).

For the FIrpic-doped films, it can be seen that FIrpic doped into all the hosts exhibit nearly mono-exponential decay curves (Fig. 3a) with relatively long lifetimes (τ) between 1.38 and 1.60 μs (Table 3). For the host of TCPB that possess the highest E_T among these hosts, nonradiative rate constant (k_{nr}) of the co-deposited film is $1.52 \times 10^5 \text{ s}^{-1}$, which is the smallest one among these doped films. In addition, it exhibits higher PL quantum efficiency (η_{PL}) of 77% than the other two, which can be attributed to more efficient energy transfer from the host to the guest and good confinement of triplet energy on the FIrpic molecules. Moreover, simultaneous PL spectra of all the co-deposited films feature emission bands at 475 and 510 nm, which are identical to the photoluminescent bands of FIrpic, indicating the emission directly from the triplet excited state of FIrpic (Figure S1a \dagger).

Ir(PPy) $_3$ doped into TCPB, TCPY, and TCPM also exhibit nearly mono-exponential decay curves with lifetimes between 1.17 and 1.26 μs and high η_{PL} of about 84%. Their radiative rate constants (k_r) are between 6.67×10^5 and $7.18 \times 10^5 \text{ s}^{-1}$, and k_{nr} s are between 1.19×10^5 and $1.37 \times 10^5 \text{ s}^{-1}$. Both are slightly influenced by the different hosts. Photoluminescent spectra of these co-deposited films feature an emission band at 520 nm with a shoulder at 550 nm, which are identical to the photoluminescent bands of Ir(PPy) $_3$ (Figure S1b \dagger).

For Ir(piq) $_3$ with the lowest triplet energy among these phosphorescent emitters, all the co-deposited films clearly exhibit almost identical mono-exponential decay curves and relatively long lifetimes of about 1.15 μs . They also show η_{PL} of 54%, which is the highest level for the Ir(piq) $_3$ -doped films reported previously. Their k_r and k_{nr} are also slightly affected by the change of the central arylene. In addition, they also show identical photoluminescent spectra (Figure S1c \dagger), which originate from the relaxation of the triplet excited states of Ir(piq) $_3$. The transient PL observation indicates that the triplet energy transfer from the

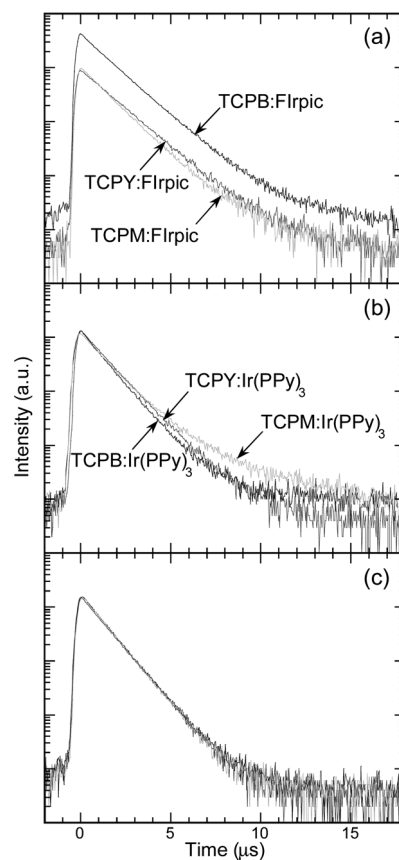


Fig. 3 Transient photoluminescence decay curves for the blue (FIrpic) (a), green (Ir(PPy) $_3$) (b), and red (Ir(piq) $_3$) (c) triplet emitters co-deposited with TCPB, TCPY, and TCPM.

general blue, green, and red phosphors to all the hosts is successfully suppressed and the energy is well-confined on the phosphor molecules due to higher E_T of the hosts than the guests although slightly decreased E_T is obtained with introducing heterocycles as the core.

Since the charge carriers are recombined in the EML in an OLED, balanced carrier injection and transport into the EML is a prerequisite for improved device performance. As thus, different from the hole-transport or electron-transport materials, balanced hole and electron mobility is ideal for a host material. Hole/electron mobilities of the hosts were measured by using

Table 3 Phosphorescence lifetime (τ), photoluminescence quantum efficiency (η_{PL}), radiative and nonradiative rate constants (k_r and k_{nr}) of FIrpic, Ir(PPy) $_3$, and Ir(piq) $_3$ co-deposited with TCPB, TCPY, and TCPM

Guests	Hosts	τ (μs)	η_{PL} (%)	k_r ($\times 10^5 \text{ s}^{-1}$)	k_{nr} ($\times 10^5 \text{ s}^{-1}$)
FIrpic	TCPB	1.51	77	5.08	1.52
	TCPY	1.60	72	4.50	1.75
	TCPM	1.38	72	5.22	2.03
Ir(PPy) $_3$	TCPB	1.17	84	7.18	1.37
	TCPY	1.26	85	6.73	1.19
	TCPM	1.24	83	6.67	1.37
Ir(piq) $_3$	TCPB	1.14	54	4.72	4.03
	TCPY	1.15	54	4.69	3.99
	TCPM	1.13	53	4.67	4.15

a conventional photo-induced time-of-flight (TOF) technique using a nitrogen laser as an excitation source ($\lambda = 337$ nm). Fig. 4 shows their hole (μ_h) and electron (μ_e) mobilities plotted as a function of the square root of the electric field (E). In general, the electron mobility of many hosts is much lower than the hole mobility because of the fact that they mainly consist of strong electron donors, like aromatic amines or carbazoles. As an example, μ_h of 1,3-bis(3-(carbazol-9-yl)phenyl)benzene (DCzPB),³⁴ a host material without any heterocycles, is one order of magnitude higher than its μ_e . Similarly, μ_h of the carbazole-based host material TCPB lies in the range from 2.4×10^{-5} to $4.1 \times 10^{-5} \text{ cm}^2 \text{ V}^{-1} \text{ s}^{-1}$ at an electric field between 7.2×10^5 and $1.0 \times 10^6 \text{ V cm}^{-1}$, which is five times higher than its μ_e , ranging from 4.6×10^{-6} to $8.5 \times 10^{-6} \text{ cm}^2 \text{ V}^{-1} \text{ s}^{-1}$ at an electric field between 5.6×10^5 and $1.0 \times 10^6 \text{ V cm}^{-1}$, which can be attributed to the carbazole moiety. In contrast, with introducing a pyridine ring instead of the central benzene, two orders of magnitude higher μ_e in the range from 3.8×10^{-4} to $4.7 \times 10^{-4} \text{ cm}^2 \text{ V}^{-1} \text{ s}^{-1}$ was achieved for TCPY at an electric field between 6.4×10^5 and $1.0 \times 10^6 \text{ V cm}^{-1}$. In addition, most importantly, its μ_h is quite similar to its μ_e , suggesting that TCPY behaves more like a bipolar host material. Similar phenomenon was also found for TCPM, but its μ_h and μ_e are nearly one order of magnitude lower than those of TCPY, but higher than those of TCPB. It is anticipated that improved carrier injection, transport, and recombination in the EML based on TCPY and TCPM should be achieved due to their improved carrier mobility and bipolarity. Compared with the host materials with the same heterocyclic core and two phenyl carbazole arms,³⁴ hole/electron mobilities of TCPY and TCPM are one order of magnitude higher. Moreover, they behave more like a bipolar host material because of their similar μ_h and μ_e .

RGB phosphorescent OLEDs were fabricated by doping Ir(piq)₃, Ir(ppy)₃, and FIrpic into the developed host materials as the EMLs, respectively. For the blue phosphorescent OLEDs based on FIrpic, the highest efficiency was achieved for the device based on TCPB, giving a maximum external quantum efficiency (η_{ext}) of 26.0% and a maximum power efficiency (η_{P}) of 65.4 lm W⁻¹, which rolls to 20.5%, 39.3 lm W⁻¹ and 17.3%, 27.1 lm W⁻¹ at 100 and 1000 cd m⁻², respectively (Table 4). In comparison, slightly lower efficiencies of 19.5% and 36.2 lm W⁻¹ were obtained at 100 cd m⁻² for the device based on TCPY. For the

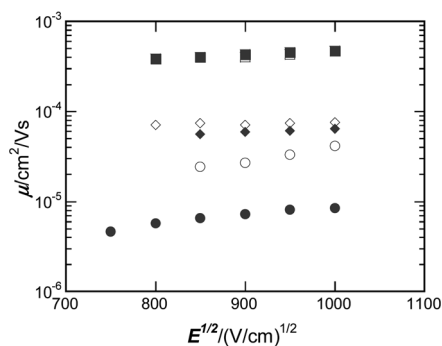


Fig. 4 Hole (μ_h) (open) and electron (μ_e) (closed) mobilities of the neat films for TCPB (●○), TCPY (■□), and TCPM (◆◇) plotted as a function of the square root of the electric field (E).

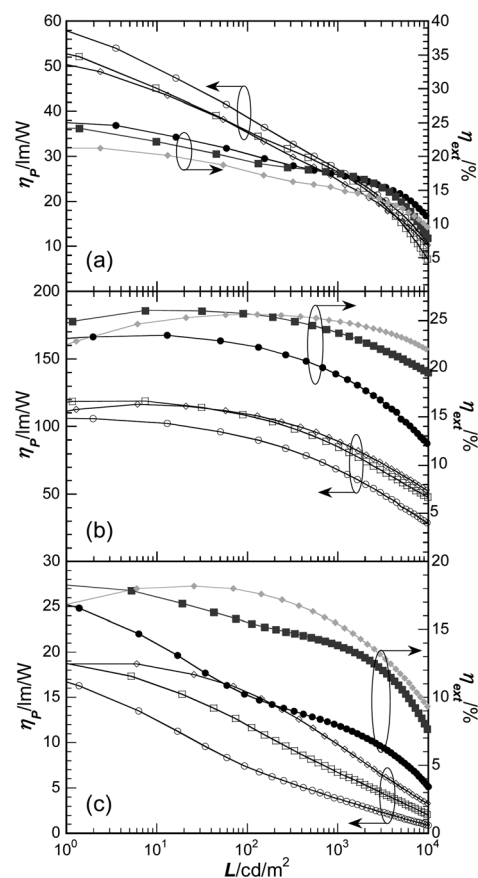


Fig. 5 External quantum efficiency (η_{ext}) (closed) and power efficiency (η_{P}) (open) vs. luminance (L) characteristics of the RGB phosphorescent OLEDs in structures: (a) ITO/TPDPES:TBAH (20 nm)/3DTAPBP (30 nm)/host:11 wt% FIrpic (10 nm)/BP4mPy (40 nm)/LiF (0.5 nm)/Al (100 nm); (b) ITO/TPDPES:TBAH (20 nm)/TAPC (30 nm)/host:8 wt% Ir(ppy)₃ (10 nm)/TmPyBPZ (50 nm)/LiF (0.5 nm)/Al (100 nm); (c) ITO/TPDPES:TBAH (20 nm)/TAPC (35 nm)/host:4 wt% Ir(piq)₃ (10 nm)/TmPyBPZ (65 nm)/LiF (0.5 nm)/Al (100 nm). Host: TCPB (○●), TCPY (□■), and TCPM (◇◆).

device based on TCPM with a pyrimidine core, the efficiencies at 100 cd m⁻² are 18.0% and 35.9 lm W⁻¹. The reduced efficiency may be partly attributed to the lower η_{PL} of the co-deposited films of TCPY:FIrpic and TCPM:FIrpic in comparison to TCPB:FIrpic. Compared with the devices based on the corresponding two-arm compounds in a similar device architecture, the efficiencies of the devices based on TCPB and TCPY are somewhat lower than those of the devices based on DCzPB and 26DCzPPy, and it can be attributed to the lower η_{PL} of the co-deposited films. However, the efficiencies of the devices based on TCPY and TCPM are much higher than those of the devices based on 24DCzPPy, 24DCzPPm, and 46DCzPPm due to the improved bipolarity and thus the improved carrier balance.³⁴ Considering the reduced LUMO energy level and improved electron mobility of TCPY and TCPM, there should be a reduced carrier balance for the devices based on TCPY and TCPM. Note that FIrpic is a well-known electron-transport triplet emitter and the concentration of FIrpic is relatively high (11 wt%). The electrons may be partly injected into the EML through the FIrpic molecules. It is shown in Figure S2a† that the current density for

Table 4 Performance data of the RGB phosphorescent OLEDs using TCPB, TCPY, and TCPM as the host materials

Guests	Hosts	Maximum efficiency		at 100 cd m ⁻²			at 1000 cd m ⁻²		
		PE (lm W ⁻¹)	η_{ext} (%)	V (V)	PE (lm W ⁻¹)	η_{ext} (%)	V (V)	PE (lm W ⁻¹)	η_{ext} (%)
FIrpic	TCPB	65.4	26.0	3.68	39.3	20.5	4.49	27.1	17.3
	TCPY	56.2	24.4	3.72	36.2	19.5	4.56	26.5	17.5
	TCPM	51.9	21.2	3.69	35.9	18.0	4.49	24.9	15.2
Ir(PPy) ₃	TCPB	107	23.4	2.76	92.3	22.5	3.21	68.2	19.4
	TCPY	119	26.0	2.71	108	25.7	3.19	84.8	23.7
	TCPM	116	25.6	2.66	109	25.6	3.18	89.1	24.9
Ir(piq) ₃	TCPB	19.8	18.6	3.83	7.3	10.2	5.71	3.83	7.93
	TCPY	19.3	18.4	3.54	12.0	15.5	5.60	6.72	13.8
	TCPM	18.7	18.2	3.08	15.6	17.8	4.25	9.80	15.4

these devices is quite similar regardless of the change of the host. The slightly reduced efficiency for the devices based on TCPY and TCPM should also be attributed to the reduced carrier balance recombined in the EML. EL spectra of the blue phosphorescent OLEDs based on TCPB, TCPY, and TCPM peak at 473 nm with a shoulder at 500 nm, which are identical to those reported previously, indicating the emission directly from the excited state of FIrpic (Figure S3a†).^{35,37}

For the green phosphorescent OLEDs, reduced driving voltages were achieved for the devices based on TCPY and TCPM in comparison to the device based on TCPB, especially at brightness lower than 1000 cd m⁻². Considering the reduced LUMO energy level and improved electron mobility of TCPY and TCPM, it indicates more carriers should be injected into the EML through the host molecules. In addition, the highest efficiency was achieved for TCPM, exhibiting η_{ext} of 25.6% and η_{P} of 109 lm W⁻¹ at 100 cd m⁻². Although the electron-transport materials utilized are different to give a different driving voltage, its η_{ext} values are higher than those of the devices based on the corresponding two-arm compounds of 24DCzPPm and 46DCzPPm due to the improved bipolarity and thus the improved carrier balance.³⁴ In addition, η_{ext} values of the devices based on TCPB and TCPY are also comparable to those of the devices based on the corresponding two-arm compounds of DCzPB, 26DCzPPy, and 24DCzPPy. Although η_{PL} of Ir(PPy)₃ doped into TCPB, TCPY, and TCPM are quite similar, the improved efficiency achieved for the hosts of TCPY and TCPM with heterocyclic cores can be attributed to their lower-lying LUMO energy levels and improved bipolarity compared with TCPB, leading to an improved electron injection and transport and thus an improved carrier balance. In addition, besides the high efficiency achieved by the host of TCPM, its η_{ext} roll very slightly from a display-relevant luminance of 100 cd m⁻² to an illumination-relevant luminance of 1000 cd m⁻². Even at a much brighter luminance of 10 000 cd m⁻², η_{ext} remains 21.9% for the device based on TCPM, compared with 12.1% and 19.6% for the devices based on TCPB and TCPY, respectively (Fig. 5). Similar to the blue phosphorescent OLEDs, EL spectra of the green phosphorescent OLEDs based on TCPB, TCPY, and TCPM peak at 515 nm with a shoulder at 550 nm, and they are identical with those reported previously.^{38,39}

For the red phosphorescent OLEDs, all the devices show very high maximum η_{ext} over 18% and maximum η_{P} as ~19 lm W⁻¹ at low current density. Considering the similar η_{PL} values of the co-deposited films of host:Ir(piq)₃, similar carrier balances is

achieved at low driving voltages. With an increase of current density, a steep decrease of η_{ext} was found for the device based on TCPB. The steep decrease in η_{ext} can be attributed to the reduced carrier balance at high current density. Considering relatively low-lying LUMO (3.40 eV) and high-lying HOMO (5.40 eV) energy levels of Ir(piq)₃, it is generally thought that carriers are injected into the EML through the Ir(piq)₃ molecules. However, note that the concentration of Ir(piq)₃ is as low as 4 wt%. At low current density, carriers may be injected into the EML through the Ir(piq)₃ molecules due to its lower-lying LUMO and higher-lying HOMO energy levels compared with the hosts. But at high current density, more carriers must be injected into the EML through the host molecules. Relatively high-lying LUMO energy level and low electron-mobility of TCPB indicate that TCPB more likely behaves as a hole-transporter and thus facilitate hole-injection and transport into the EML to give a reduced carrier balance. The reduced carrier balance induces decreased carrier recombination efficiency and thus reduced η_{ext} . In addition, the imbalance of the carriers also causes domination of hole polaron (*h*⁺), and a large number of holes and polarons accumulate at the interface of EML and ETL and/or in the active layer, resulting in triplet exciton–polaron quenching and thus further efficiency roll-off.⁴⁰ On this result, η_{ext} rolls off to 10.2% at 100 cd m⁻² and 7.93% at 1000 cd m⁻². Besides the reduced carrier balance, relatively high driving voltages of 3.83 and 5.71 V were obtained at 100 and 1000 cd m⁻², respectively, which can be attributed to the high-lying LUMO energy level and low electron mobility of TCPB and thus a high electron injection barrier from the electron transport layer. Due to high driving voltages, η_{P} further rolls off to 7.30 lm W⁻¹ at 100 cd m⁻² and 3.83 lm W⁻¹ at 1000 cd m⁻². On this reason, similar steep decreases in η_{ext} and η_{P} have also been found for the other host materials based on carbazole building blocks, like CBP.³⁴

Although efficiency roll-off was also found for the device based on TCPY, it was significantly suppressed compared with the device based on TCPB, giving η_{ext} values of 15.5% and 13.8% and η_{P} values of 12.0 and 6.72 lm W⁻¹ at 100 and 1000 cd m⁻², respectively. Compared with the devices based on the host materials containing a pyridine core and two phenyl carbazole arms, efficiency roll-off was also significantly suppressed, giving improved η_{ext} and η_{P} (Figure S4a†). The suppressed efficiency roll-off can be attributed to its lower-lying LUMO energy level and improved bipolarity, giving improved carrier balance and thus suppressed triplet exciton–polaron quenching at high current density. Besides the improved efficiency, reduced driving

voltage was also achieved for the device based on TCPY in comparison with the device based on TCPB, which can be attributed to its lower-lying LUMO energy level, smaller ΔE_{ST} , and increased carrier mobility (Figure S2c†).

Efficiency roll-off was further suppressed for the device based on TCPM with a pyrimidine core, giving η_{ext} values of 17.8% and 15.4% and η_P values of 15.6 and 9.80 lm W⁻¹ at 100 and 1000 cd m⁻², respectively, which is one of the highest efficiencies for the Ir(piq)₃-based red phosphorescent OLEDs.^{41–44} Moreover, further decreased driving voltages of 3.08 and 4.25 V were achieved at 100 and 1000 cd m⁻², respectively, which are even equal to or lower than those of the devices based on a *p-i-n* architecture,^{43,44} and it can be attributed to its further decreased LUMO energy level, narrower E_g , and smaller ΔE_{ST} achieved with introducing pyrimidine as the core. The reduced driving voltage achieved with the change of host material further proves that more carriers must be injected into the EML through the host molecules rather than direct carrier trap by the dopant, especially at high current density. In addition, the device based on TCPM exhibits a lower driving voltage compared with the devices based on the host materials containing a pyrimidine core and two phenyl carbazole arms due to its high hole/electron mobilities. Although a slightly lower η_{ext} is achieved at a luminance higher than 800 cd m⁻², its η_P is still higher than the other two due to the reduced driving voltage (Figure S4b†). The emission color is deep red with an EL emission peak at 621 nm and Commission Internationale de L'Éclairage (CIE) color coordinates of (0.67, 0.33), independent of the choice of hosts. This proves the emission directly from the triplet emitter Ir(piq)₃.

Experimental

Characterization

All the developed host materials were purified by silica gel chromatography and then repeated thermal gradient vacuum sublimation before characterization and device fabrication. ¹H and ¹³C NMR spectra were recorded on a Varian 500 (500 MHz) spectrometer. Mass spectra were obtained using a JEOL JMS-K9 mass spectrometer. Elemental analysis was performed on a Vario EL elemental analysis instrument (Elementar Co.). Differential scanning calorimetry (DSC) was performed using a Perkin-Elmer Diamond DSC Pyris instrument under a nitrogen atmosphere at a heating rate of 10 °C min⁻¹. Thermogravimetric analysis (TGA) was undertaken using a SEIKO EXSTAR 6000 TG/DTA 6200 unit under a nitrogen atmosphere at a heating rate of 10 °C min⁻¹. UV-Vis spectra were measured using a Shimadzu UV-3150 UV-vis-NIR spectrophotometer. Steady-state PL spectra were obtained at room temperature using a FluoroMax-2 (Jobin-Yvon-Spex) luminescence spectrometer. Ionization potentials were determined by atmospheric ultraviolet photoelectron spectroscopy (Rikken Keiki AC-3). Time-resolved emission spectra were obtained at $T = 4.2$ K under excitation by a nitrogen laser ($\lambda = 337$ nm, 50 Hz, 800 ps pulses) combined with a streak scope C4334 (Hamamatsu) and a synchronous delay generator C4792-02 (Hamamatsu). In comparison, transient PL decays and the corresponding simultaneous PL spectra of the phosphorescent emitter-doped films were recorded at room temperature. PL quantum efficiencies of the co-deposited films

were measured by using an integrating sphere under nitrogen gas flow at room temperature.

Calculations

Density functional theory (DFT) calculations were performed by using the Gaussian suite of programs (Gaussian 03W). For the calculation of HOMO and LUMO energy levels, the ground state structures were optimized at the restricted B3LYP/6-31G(d) level, and the single-point energies were calculated at the restricted B3LYP/6-311+G(d,p) level. The ground state (S_0) structure optimization and single-point energy calculation were performed at the B3LYP/6-31G(d) level. In contrast, the lowest-energy triplet excited state (T_1) structure optimization and single-point energy calculation were performed at the unrestricted B3LYP/6-31G(d) level.⁴⁵

Device fabrication and characterization

Phosphorescent OLEDs were grown on glass substrates pre-coated with a ~110-nm-thick layer of indium-tin oxide (ITO) having a sheet resistance of 15 Ω/\square . The substrates were cleaned with ultrapurified water and organic solvents and then dry-cleaned for 20 min by exposure to an UV-ozone ambient. To improve the hole injection from the anode, poly(arylene amine ether sulfone)-containing tetraphenylbenzidine (TPDPES) doped with 10% (by weight) tris(4-bromophenyl) aminium hexachloroantimonate (TBPAH) was spun onto the precleaned substrate from its dichloroethane solution to form a 20-nm-thick polymer buffer layer.⁴⁶ For the red phosphorescent OLEDs, a 35-nm-thick 1,1-bis(4-(*N,N*-di(*p*-tolyl)-amino)phenyl)-cyclohexane (TAPC) was deposited onto the buffer layer as a hole-transport layer (HTL). Then, 4% (by weight) Ir(piq)₃ was co-deposited with the host materials to form a 10-nm-thick EML. Finally, a 65-nm-thick electron-transport layer (ETL) of 2,4,6-tris(3'-(pyridin-2-yl)biphenyl-3-yl)-1,3,5-triazine (TmPyBPZ)³⁸ was deposited to block holes and to confine excitons in the emissive zone. For the green phosphorescent OLEDs, TAPC (30 nm), Ir(PPy)₃ (7 wt%):host (10 nm), and TmPyBPZ (50 nm) were successively deposited as the HTL, EML, and ETL, respectively. 2,2'-Bis(*m*-di-*p*-tolylaminophenyl)-1,1'-biphenyl (3DTAPBP) (30 nm), FIrpic (11 wt%):host (10 nm), and 3,5,3',5'-tetra(*m*-pyrid-3-yl)phenyl-(1,1')-biphenyl (BP4mPy)³⁹ (40 nm) were successively deposited as the HTL, EML, and ETL, respectively, for the blue phosphorescent OLEDs. Molecular structures and acronyms of the materials used for device fabrication are shown in Scheme S2.† Cathodes consisting of a 0.5-nm-thick layer of LiF followed by a 100-nm-thick layer of Al were patterned using a shadow mask with an array of 2 mm × 2 mm openings. The electroluminescent (EL) spectra were recorded by an optical multichannel analyzer, Hamamatsu PMA 11. The current density and luminance *versus* driving voltage characteristics were measured by Keithley source-measure unit 2400 and Konica Minolta chroma meter CS-200, respectively. η_{ext} is calculated from the luminance, current density, and EL spectra, assuming a Lambertian distribution.

For the carrier mobility measurement, neat films of host materials (~10 μ m) were vacuum-deposited on ITO-coated substrates. A semi-transparent Al layer was patterned using

a shadow mask with an array of 2 mm × 2 mm openings. The hole/electron mobilities were measured by using a conventional photo-induced TOF technique. A nitrogen laser was used as the excitation source ($\lambda = 337$ nm) and was incident on the sample through the ITO or semi-transparent Al electrode.

Conclusion

We report a series of star-shaped host materials containing various arylene cores, like benzene, pyridine, and pyrimidine, for RGB phosphorescent OLEDs. Reduced LUMO energy levels are achieved by introducing heterocyclic cores of pyridine and pyrimidine instead of benzene, and the more nitrogen atoms in the heterocyclic core, the lower-lying LUMO energy level is achieved. In addition, narrower energy band gaps, lower energy singlet and triplet excited states, smaller energy difference ΔE_{ST} , and improved bipolarity are also achieved with the hosts containing a heterocyclic core. Compared with the slightly reduced E_T , the significantly decreased ΔE_{ST} achieved with introducing heterocyclic arylens as the core indicates that introducing appropriate electron donors and acceptors as building blocks of a host material may be an effective route to give attractive candidate for phosphorescent OLEDs with reduced driving voltage as well as good triplet exciton confinement. As a result, reduced driving voltage was achieved for the green and red phosphorescent OLEDs based on TCPY and TCPM, giving improved efficiency as well as suppressed efficiency roll-off.

Acknowledgements

S. J. S. greatly appreciates the financial support from the National Natural Science Foundation of China (51073057), the Ministry of Science and Technology (2009CB930604 and 2011AA03A110), and the Fundamental Research Funds for the Central Universities (2011ZZ0002).

References

- M. A. Baldo, D. F. O'Brien, Y. You, A. Shoustikov, S. Sibley, M. E. Thompson and S. R. Forrest, *Nature*, 1998, **395**, 151.
- M. A. Baldo, S. Lamansky, P. E. Burrows, M. E. Thompson and S. R. Forrest, *Appl. Phys. Lett.*, 1999, **75**, 4.
- C. Adachi, M. A. Baldo, M. E. Thompson and S. R. Forrest, *J. Appl. Phys.*, 2001, **90**, 5048.
- C. Adachi, R. C. Kwong, P. Djurovich, V. Adamovich, M. A. Baldo, M. E. Thompson and S. R. Forrest, *Appl. Phys. Lett.*, 2001, **79**, 2082.
- R. J. Holmes, S. R. Forrest, Y.-T. Tung, R. C. Kwong, J. J. Brown, S. Garon and M. E. Thompson, *Appl. Phys. Lett.*, 2003, **82**, 2422.
- S. Tokito, T. Iijima, Y. Suzuki, H. Kita, T. Tsuzuki and F. Sato, *Appl. Phys. Lett.*, 2003, **83**, 569.
- P.-I. Shih, C.-H. Chien, C.-Y. Chuang, C.-F. Shu, C.-H. Yang, J.-H. Chen and Y. Chi, *J. Mater. Chem.*, 2007, **17**, 1692.
- M.-H. Tsai, H.-W. Lin, H.-C. Su, T. H. Ke, C.-C. Wu, F.-C. Fang, Y.-L. Liao, K.-T. Wong and C.-I. Wu, *Adv. Mater.*, 2006, **18**, 1216.
- S.-J. Yeh, M.-F. Wu, C.-T. Chen, Y.-H. Song, Y. Chi, M.-H. Ho, S.-F. Hsu and C. H. Chen, *Adv. Mater.*, 2005, **17**, 285.
- X. Ren, J. Li, R. J. Holmes, P. I. Djurovich, S. R. Forrest and M. E. Thompson, *Chem. Mater.*, 2004, **16**, 4743.
- R. J. Holmes, B. W. D'Andrade, S. R. Forrest, X. Ren, J. Li and M. E. Thompson, *Appl. Phys. Lett.*, 2003, **83**, 3818.
- P.-I. Shih, C.-L. Chiang, A. K. Dixit, C.-K. Chen, M.-C. Yuan, R.-Y. Lee, C.-T. Chen, E. W.-G. Diau and C.-F. Shu, *Org. Lett.*, 2006, **8**, 2799.
- M.-H. Tsai, Y.-H. Hong, C.-H. Chang, H.-C. Su, C.-C. Wu, A. Matoliukstyte, J. Simokaitiene, S. Grigalevicius, J. V. Grazulevicius and C.-P. Hsu, *Adv. Mater.*, 2007, **19**, 862.
- H. Fukagawa, K. Watanabe, T. Tsuzuki and S. Tokito, *Appl. Phys. Lett.*, 2008, **93**, 133312.
- M.-H. Tsai, T.-H. Ke, H.-W. Lin, C.-C. Wu, S.-F. Chiu, F.-C. Fang, Y.-L. Liao, K.-T. Wong, Y.-H. Chen and C.-I. Wu, *ACS Appl. Mater. Interfaces*, 2009, **1**, 567.
- K. Brunner, A. van Dijken, H. Börner, J. J. A. M. Bastiaansen, N. M. M. Kiggen and B. M. W. Langeveld, *J. Am. Chem. Soc.*, 2004, **126**, 6035.
- Z. Jiang, Y. Chen, C. Yang, Y. Cao, Y. Tao, J. Qin and D. Ma, *Org. Lett.*, 2009, **11**, 1503.
- C.-H. Chen, W.-S. Huang, M.-Y. Lai, W.-C. Tsao, J. T. Lin, Y.-H. Wu, T.-H. Ke, L.-Y. Chen and C.-C. Wu, *Adv. Funct. Mater.*, 2009, **19**, 2661.
- S.-Y. Takizawa, V. A. Montes and P. Anzenbacher Jr., *Chem. Mater.*, 2009, **21**, 2452.
- Z. Ge, T. Hayakawa, S. Ando, M. Ueda, T. Akiike, H. Miyamoto, T. Kajita and M. Kakimoto, *Chem. Mater.*, 2008, **20**, 2532.
- Z. Ge, T. Hayakawa, S. Ando, M. Ueda, T. Akiike, H. Miyamoto, T. Kajita and M. Kakimoto, *Adv. Funct. Mater.*, 2008, **18**, 584.
- A. B. Padmaperuma, L. S. Sapochak and P. E. Burrows, *Chem. Mater.*, 2006, **18**, 2389.
- P. A. Vecchi, A. B. Padmaperuma, H. Qiao, L. S. Sapochak and P. E. Burrows, *Org. Lett.*, 2006, **8**, 4211.
- H.-F. Chen, S.-J. Yang, Z.-H. Tsai, W.-Y. Hung, T.-C. Wang and K.-T. Wong, *J. Mater. Chem.*, 2009, **19**, 8112.
- H. Inomata, K. Goushi, T. Masuko, T. Konno, T. Imai, H. Sasabe, J. J. Brown and C. Adachi, *Chem. Mater.*, 2004, **16**, 1285.
- M. M. Rothmann, S. Haneder, E. Da Como, C. Lennartz, C. Schildknecht and P. Strohhriegl, *Chem. Mater.*, 2010, **22**, 2403.
- M.-K. Leung, C.-C. Yang, J.-H. Lee, H.-H. Tsai, C.-F. Lin, C.-Y. Huang, Y. O. Su and C.-F. Chiu, *Org. Lett.*, 2007, **9**, 235.
- S.-J. Su, H. Sasabe, T. Takeda and J. Kido, *Chem. Mater.*, 2008, **20**, 1691.
- Y. Tao, Q. Wang, C. Yang, Q. Wang, Z. Zhang, T. Zou, J. Qin and D. Ma, *Angew. Chem., Int. Ed.*, 2008, **47**, 8104.
- F.-M. Hsu, C.-H. Chien, P.-I. Shih and C.-F. Shu, *Chem. Mater.*, 2009, **21**, 1017.
- S. O. Jeon, K. S. Yook, C. W. Joo and J. Y. Lee, *Adv. Funct. Mater.*, 2009, **19**, 3644.
- S. O. Jeon, K. S. Yook, C. W. Joo and J. Y. Lee, *Adv. Mater.*, 2010, **22**, 1872.
- H.-H. Chou and C.-H. Cheng, *Adv. Mater.*, 2010, **22**, 2468.
- S.-J. Su, C. Cai and J. Kido, *Chem. Mater.*, 2011, **23**, 274.
- S.-J. Su, T. Chiba, T. Takeda and J. Kido, *Adv. Mater.*, 2008, **20**, 2125.
- P. Schrögel, A. Tomkevičienė, P. Strohhriegl, S. T. Hoffmann, A. Köhlerb and C. Lennartz, *J. Mater. Chem.*, 2011, **21**, 2266.
- S.-J. Su, Y. Takahashi, T. Chiba, T. Takeda and J. Kido, *Adv. Funct. Mater.*, 2009, **19**, 1260.
- S.-J. Su, H. Sasabe, Y.-J. Pu, K.-I. Nakayama and J. Kido, *Adv. Mater.*, 2010, **22**, 3311.
- S.-J. Su, D. Tanaka, Y.-J. Li, H. Sasabe, T. Takeda and J. Kido, *Org. Lett.*, 2008, **10**, 941.
- S. Reineke, K. Walzer and K. Leo, *Phys. Rev. B: Condens. Matter Mater. Phys.*, 2007, **75**, 125328.
- T. Tsuzuki and S. Tokito, *Adv. Mater.*, 2007, **19**, 276.
- H. Kanno, K. Ishikawa, Y. Nishio, A. Endo, C. Adachi and K. Shibata, *Appl. Phys. Lett.*, 2007, **90**, 123509.
- R. Meerheim, K. Walzer, G. He, M. Pfeiffer and K. Leo, *Proc. SPIE-Int. Soc. Opt. Eng.*, 2006, **6192**, 61920P.
- R. Meerheim, K. Walzer, M. Pfeiffer and K. Leo, *Appl. Phys. Lett.*, 2006, **89**, 061111.
- Gaussian 03, Revision D.01*, M. J. Frisch, G. W. Trucks, H. B. Schlegel, G. E. Scuseria, M. A. Robb, J. R. Cheeseman, J. A. Montgomery Jr., T. Vreven, K. N. Kudin, J. C. Burant, J. M. Millam, S. S. Iyengar, J. Tomasi, V. Barone, B. Mennucci, M. Cossi, G. Scalmani, N. Rega, G. A. Petersson, H. Nakatsuji, M. Hada, M. Ehara, K. Toyota, R. Fukuda, J. Hasegawa, M. Ishida, T. Nakajima, Y. Honda, O. Kitao, H. Nakai, M. Klene, X. Li, J. E. Knox, H. P. Hratchian, J. B. Cross, V. Bakken, C. Adamo, J. Jaramillo, R. Gomperts, R. E. Stratmann, O. Yazyev,

A. J. Austin, R. Cammi, C. Pomelli, J. W. Ochterski, P. Y. Ayala, K. Morokuma, G. A. Voth, P. Salvador, J. J. Dannenberg, V. G. Zakrzewski, S. Dapprich, A. D. Daniels, M. C. Strain, O. Farkas, D. K. Malick, A. D. Rabuck, K. Raghavachari, J. B. Foresman, J. V. Ortiz, Q. Cui, A. G. Baboul, S. Clifford, J. Cioslowski, B. B. Stefanov, G. Liu, A. Liashenko, P. Piskorz,

I. Komaromi, R. L. Martin, D. J. Fox, T. Keith, M. A. Al-Laham, C. Y. Peng, A. Nanayakkara, M. Challacombe, P. M. W. Gill, B. Johnson, W. Chen, M. W. Wong, C. Gonzalez and J. A. Pople, Gaussian, Inc., Wallingford CT, 2004.
46 Y. Sato, T. Ogata and J. Kido, *Proc. SPIE-Int. Soc. Opt. Eng.*, 2000, **4105**, 134.